Characterization of Superlighting Polymer−DNA Aggregates: A Fluorescence and Light Scattering Study †

ARTICLE *in* LANGMUIR · FEBRUARY 2007

Impact Factor: 4.46 · DOI: 10.1021/la061699a · Source: PubMed

Characterization of Superlighting Polymer−DNA Aggregates: A Fluorescence and Light Scattering Study†

Kim Doré,[‡,§,||] Rodica Neagu-Plesu,[‡,||] Mario Leclerc,[‡,||] Denis Boudreau,*[,‡,§] and Anna M. Ritcey*[,‡,||]

Department of Chemistry, Centre d'optique, photonique et laser (COPL), and Centre de recherches sur la science et l'ingénierie des macromolécules (CERSIM), Université Laval, Quebec City, QC, Canada G1K 7P4

Received June 13, 2006. In Final Form: September 18, 2006

The massive amplification of fluorescence signal observed upon hybridization of as few as five DNA molecules into self-assembled structures formed between a cationic polymer and DNA oligonucleotides is investigated. These superlighting polymer−DNA aggregates were studied by fluorescence spectroscopy, static and dynamic light scattering, and zeta potential measurements in order to characterize the aggregation behavior and to understand the processes involved during DNA detection. Multi-angle laser light scattering was also used to obtain the weight-average aggregate mass (A_M), the aggregation number (N_{agg}), the radius of gyration (R_g), and the dissymmetry ratio (z). These results have been used, together with TEM imaging, to propose a suitable physical model for the aggregates.

The development of biosensors able to detect bacteria and viruses with the use of their genetic signatures has been generating increasing interest recently. For this purpose, various optical and electrochemical DNA sensors have been proposed,[1−10] most of them relying either on complex instrumentation or some form of chemical amplification (such as the polymerase chain reaction, PCR[11]) or both. We recently reported on the development of an ultrasensitive and sequence-specific DNA detection system that is particularly simple.[4,8] Basically, a cationic polymeric transducer (poly[1H-imidazolium bromide, 1-methyl-3-[2-[(4-methyl-3-thienyl)oxy]ethyl], belonging to the poly(3-alkoxy-4-methylthiophenes) class) is stoichiometrically mixed with a single-stranded DNA (ss-DNA) probe, which forms a complex (the "duplex"); when target ss-DNA is added, hybridization takes place, and the polymer seems to wrap around the double-stranded DNA (ds-DNA) in a structure called the "triplex". Interestingly, this change in polymer conformation upon hybridization is associated with an important increase in fluorescence intensity,[4] which makes possible the detection of a few hundred copies of target DNA.[8] Furthermore, we recently demonstrated that the use of Förster resonance energy transfer (FRET) between the polymer sensor and a fluorophore (Alexafluor 546) tagged on the ss-DNA probes leads to an improvement in detection sensitivity by a factor of ∼4000 and to the detection of as few as five copies of target DNA.[10,12] It has been postulated that the increase in sensitivity provided by this process (called "fluorescence chain reaction", or FCR) is made possible by the self-assembly of hundreds of polymer-labeled probe complexes in supramolecular aggregates with a geometry that favors fast energy transfer between FRET donors and acceptors.[12]

In the present work, these aggregates are studied by fluorescence spectroscopy, static and dynamic light scattering, and zeta potential measurements. The role played by aggregation in determining the luminescence properties of the unlabeled system is shown, as well as the micellar character of labeled aggregates. Moreover, results from measurements of micelle hydrodynamic size and zeta potential as a function of the number of perfectly matched DNA targets, targets having one mismatch, or NaCl added are discussed. Important information about the shape of supramolecular aggregates has also been retrieved from multi-angle laser light scattering (MALLS).[13−15] The weight-average aggregate mass (A_M), aggregation number (N_{agg}), radius of gyration (R_g), and dissymmetry ratio (z) values determined with this technique have been used, together with TEM microscopy, to build a suitable physical model of the aggregates. Ultimately, these studies will lead to an improved understanding of the processes involved in the FCR process and to improved robustness and reproducibility of this DNA-sensing system.

Materials and Methods

Materials. The polymeric transducer was synthesized according to a previously published procedure.[4,8] Unlabeled oligonucleotides and oligonucleotides labeled with Alexafluor 546 (referred to as

† Part of the Stimuli-Responsive Materials: Polymers, Colloids, and Multicomponent Systems special issue.

* Corresponding authors. E-mail: denis.boudreau@chm.ulaval.ca, anna.ritcey@chm.ulaval.ca.

‡ Department of Chemistry.

§ Centre d'optique, photonique et laser (COPL).

|| Centre de recherches sur la science et l'ingénierie des macromolécules (CERSIM).

(1) Tyagi, S.; Kramer, F. R. *Nat. Biotechnol.* **1996**, *14*, 303−308.

(2) Dubertret, B.; Calame, M.; Libchaber, A. J. *Nat. Biotechnol.* **2001**, *19*, 365−370.

(3) Gaylord, B. S.; Heeger, A. J.; Bazan, G. C. *Proc. Nat. Acad. Sci. U.S.A.* **2002**, *99*, 10954−10957.

(4) Ho, H. A.; Boissinot, M.; Bergeron, M. G.; Corbeil, G.; Dore, K.; Boudreau, D.; Leclerc, M. *Angew. Chem., Int. Ed.* **2002**, *41*, 1548−1551.

(5) Drummond, T. G.; Hill, M. G.; Barton, J. K. *Nat. Biotechnology* **2003**, *21*, 1192−1199.

(6) Wang, J.; Polsky, R.; Merkoci, A.; Turner, K. L. *Langmuir* **2003**, *19*, 989−991.

(7) Liu, B.; Bazan, G. C. *Chem. Mater.* **2004**, *16*, 4467−4476.

(8) Dore, K.; Dubus, S.; Ho, H. A.; Levesque, I.; Brunette, M.; Corbeil, G.; Boissinot, M.; Boivin, G.; Bergeron, M. G.; Boudreau, D.; Leclerc, M. *J. Am. Chem. Soc.* **2004**, *126*, 4240−4244.

(9) Nam, J.-M.; Stoeva, S. I.; Mirkin, C. A. *J. Am. Chem. Soc.* **2004**, *126*, 5932−5933.

(10) Ho, H. A.; Dore, K.; Boissinot, M.; Bergeron, M. G.; Tanguay, R. M.; Boudreau, D.; Leclerc, M. *J. Am. Chem. Soc.* **2005**, *127*, 12673−12676.

(11) Saiki, R. K.; Scharf, S.; Faloona, F.; Mullis, K. B.; Horn, G. T.; Erlich, H. A.; Arnheim, N. *Science* **1985**, *230*, 1350−1354.

(12) Dore, K.; Leclerc, M.; Boudreau, D. *J. Fluoresc.* **2006**, *16*, 259−265.

(13) Fuetterer, T.; Nordskog, A.; Hellweg, T.; Findenegg, G. H.; Foerster, S.; Dewhurst, C. D. *Phys. Rev. E* **2004**, *70*, 041408.

(14) Appell, J.; Porte, G. *J. Colloid Interface Sci.* **1981**, *81*, 85−90.

(15) Ishizu, K.; Toyoda, K.; Furukawa, T.; Sogabe, A. *Macromolecules* **2004**, *37*, 3954−3957.

10.1021/la061699a CCC: $37.00
Published on Web 11/30/2006

AF546 in the text) were both purchased from Integrated DNA Technologies. For all experiments, DNA capture probes consisted of a 15-mer sequence specific to the human genomic IVS12 mutation responsible for the hereditary disease *tyrosinemia*, TAN 100: 5′-CCG GTG AAT ATC TGG-3′, with the target sequence being its perfect complementary sequence, TAN 100a: 3′-GGC CAC TTA TAG ACC-5′.[10] The studies involving 1-mismatch targets were done with the capture probe sequence TAN 101: 5′-CCG GTG A**G**T ATC TGG-3′ and the same target sequence, TAN 100a.[10] Cresyl violet (CV in the text) acetate dye (65%) was purchased from Sigma-Aldrich. All dilutions and solution handling were performed in sterilized water and plasticware.

Hybridization Conditions. For all studies involving DNA hybridization, stoichiometric quantities (on a monomeric basis) of polymer and oligonucleotide capture probes were mixed, and the resulting solution was diluted in pure water to the desired concentration after an equilibration period of at least 60 s to allow for electrostatic complexation. The solution was then heated to 50 °C. Following another equilibration period of 5 min, target DNA was added. Although less than 5 min is needed for hybridization to occur at the concentration level used for the present work ($\sim 10^{-7}$ M polymer−probe complex), an additional equilibration period of 5 min (10 min total) was added to ensure complete and stable complex formation. For the unlabeled system, hybridization was done in 0.1 M NaCl; for the labeled system, hybridization was performed in sterilized Nanopure water. Detailed information on these experimental procedures can be found in refs 4 and 8 for the unlabeled system and in ref 10 for the labeled system.

Light-Scattering Experiments. *Static Light Scattering.* Static light scattering measurements were performed with a DAWN laser photometer (model DSP) using the 90° detector. This instrument was also used to determine the weight-average mass of the aggregates (A_M) by multi-angle laser light scattering (MALLS) using all 18 detectors and the DAWN software and procedure provided by the manufacturer. Measurements made between 38 and 147° were used for the calculations, and the concentration of the polymer−probe complex was varied from 5.2×10^{-7} to 4.07×10^{-6} g/mL. The absence of deleterious effects due to fluorescence on scattered light intensity was verified by confirming that the insertion of a bandpass filter centered at 633 nm in front of the MALLS detectors resulted in no change in signal. The Debye formalism was used for the calculation of A_M, R_g (gyration radius), and A_2 (second virial coefficient). Berry and Zimm models were also considered but resulted in significantly larger errors in the numerical values obtained. Prior to the MALLS measurements, the specific refractive index increment d*n*/d*C*, which must be known very precisely because the calculated molecular weight scales as (d*n*/d*C*),[2] was determined with a Wyatt Optilab interferometric refractometer (model 903) using bovine serum albumin (BSA) as a standard. Care was taken to clean the refractometer cell between each measurement with nitric acid to avoid contamination from BSA adhesion. All measurements were carried out at an incident wavelength of 633 nm, at room temperature, and in pure, sterilized, filtered (0.45 μm) water.

Dynamic Light Scattering. Dynamic light scattering measurements were performed with a Zetasizer Nano ZS (ZEN 3600) instrument. Sizes were determined using the *Z*-average parameter throughout this work with the exception of the data in Table 2 and Figure 3, for which particle size distributions were evaluated from intensity measurements. All size values are the average of at least 3 different measurements of 15 runs each. All measurements were taken in pure, sterilized, filtered (0.45 μm) water at 50 °C except for the temperature-dependent sizes reported in Table 1.

Fluorescence Experiments. Fluorescence measurements were performed on a Varian Cary-Eclipse spectrofluorimeter. For Figure 1, the excitation wavelength was 425 nm, and the emission wavelength was 530 nm (the fluorescence maximum for the free polymer). For the energy-transfer measurements reported in Figure 2, the excitation wavelength was either 425 nm (for the polymer−DNA + CV samples) or 546 nm (for the AF546−DNA + CV solution), and the emission wavelength was measured at both 575 nm (the emission maximum for AF546) and 638 nm (the emission maximum for CV).

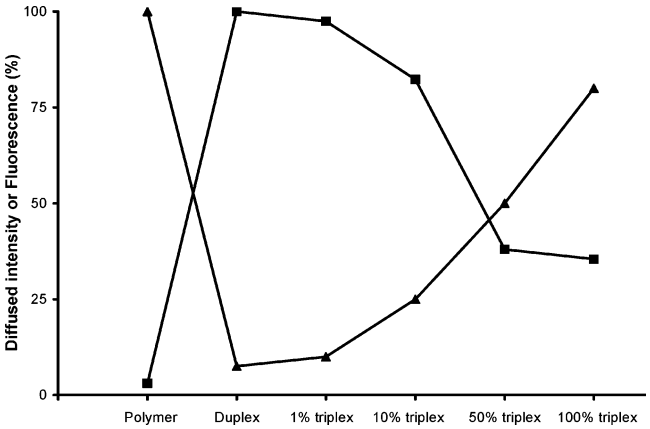

Figure 1. Fluorescence intensity (▲) and static light scattering intensity (■) of the unlabeled system upon detection of perfectly complementary DNA. For the fluorescence measurements, $\lambda_{exc} =$ 425 nm and $\lambda_{em} = 530$ nm. The scattered light was recorded at 90°.

The FRET efficiency (*E*) was calculated from

$$E = 1 - \frac{F_{da}}{F_d}$$

where F_{da} and F_d are the fluorescence intensities of the donor in the presence and absence of the acceptor, respectively, according to Lakowicz.[16] The excitation and emission slits were set at 10 nm for all data taken, and all measurements were carried out at 50 °C.

Zeta Potential Experiments. Zeta potential measurements were performed with a Zetasizer NanoZS instrument using a standard dip cell. All data points correspond to an average over 5 measurements of 30 runs each. The average electric field strength was 2500 V/m, and all measurements were carried out at 50 °C.

Transmission Electron Microscopy (TEM). TEM images were acquired with a JEOL 1230 transmitting electron microscope. Measurements were carried out on Formvar-coated (Fluka-Bio-Chemika) nickel grids from Canemco. Polymer−DNA aggregates were deposited on the grids after 20 min of ultrasonic treatment and were then allowed to dry for 2 h. Osmium tetroxyde staining was then performed with a drop of 0.1% solution (Sigma-Aldrich, OsO_4 4%) deposited on each of the grids, which were finally allowed to dry overnight.

Results and Discussion

Figure 1 shows the static light scattering intensity measured at 90° for the free polymer in solution as well as for solutions containing unlabeled polymer−probe complexes (duplexes) to which various amounts of DNA target have been added. The fluorescence intensity recorded for the same samples is also shown. There is a clear correlation between the two parameters, suggesting that the fluorescence intensity emitted by the complexes is closely related to their aggregation properties. The polymer alone is highly fluorescent and is also highly water-soluble because of the positive charge present on each repeat unit; the corresponding scattering intensity is thus very low. The polymer−DNA probe complex (duplex) is only weakly fluorescent, whereas the scattered light intensity is high because duplexes aggregate in aqueous solution as a result of their overall neutral state. Upon incremental introduction of target DNA, hybridization occurs, leading to triplex formation and to an increase in fluorescence intensity (i.e., the change in fluorescence that forms the basis for the DNA detection scheme). As shown in Figure 1, triplex formation is associated with a decrease in

(16) Lakowicz, J. R. *Principles of Fluorescence Spectroscopy*, 2nd ed.; Kluwer Academic/Plenum: New York, 1999.

Table 1. Size of Labeled and Unlabeled Duplex Aggregates at Different Temperatures[a]

temperature (°C)	mean size of unlabeled aggregates (nm)	mean size of labeled aggregates (nm)
25	397	78
40	197	80
55	116	90
65	104	111

[a] The concentration of the polymer−probe complex is $\sim 10^{-7}$ M.

light scattering intensity because duplex aggregates dissolve as they become charged.

These results suggest that aggregated complexes become fluorescent only upon dissolution, a behavior that has also been observed by Inganäs[17] for polythiophene derivatives. However, it has been postulated that the FRET-enhanced fluorescence observed with the labeled system (the FCR system) could be due to an aggregation of labeled probe−polymer complexes that maintains the donor and acceptor moieties in close proximity in an aggregated state that persists upon hybridization.[12] For this hypothesis to be valid, labeled triplexes should differ significantly from unlabeled ones.

The size of labeled and unlabeled duplex aggregates, as determined by dynamic light scattering, is presented in Table 1 as a function of temperature. Important differences between the two systems are evident. At 25 °C, unlabeled aggregates are about 5 times larger than labeled ones. Perhaps more significant is the dependence of aggregate size on temperature. The mean diameter of labeled aggregates increases with increasing temperature whereas the size of unlabeled aggregates decreases. A decrease in aggregate size upon heating would be expected for any precipitated solute. The behavior observed for the labeled system, however, indicates that the aggregation process is primarily driven by entropy. Such behavior is characteristic of micellar structures[18] that form because of hydrophobicity. In other words, aggregation takes place to diminish the organization of water molecules around the hydrophobic parts of labeled polymer−DNA complexes.

In addition to the differences shown in Table 1, it is important to note that labeled and unlabeled systems also differ with respect to particle size distribution. Typically, particle size distributions are broader and repeatability is poorer for the unlabeled system. These observations also support the hypothesis of a micellelike structure for the labeled system that exhibits a defined characteristic size. To investigate the micellar behavior of labeled aggregates further, a Förster resonance energy transfer (FRET) study was undertaken. In this experiment, cresyl violet (CV) dye was added in various concentrations to solutions containing labeled duplex aggregates, with and without added target DNA. CV can act as a FRET acceptor and absorb the fluorescence emitted by AF546 if the two fluorophores are in close proximity. Because CV has a charged polyaromatic structure like AF546, it should therefore be co-located with AF546 units within the micellelike structures. Figure 2 shows the AF546-CV FRET efficiency as a function of the CV/AF546 molar ratio. For this experiment, the AF546 concentration was kept constant ($\sim 10^{-7}$ M) while CV was added successively for each data point, and the optical density of the samples at 575 nm was kept below 0.02 to avoid inner filter effects. For comparison, results are also shown for the two dyes free in solution. As shown in Figure 2,

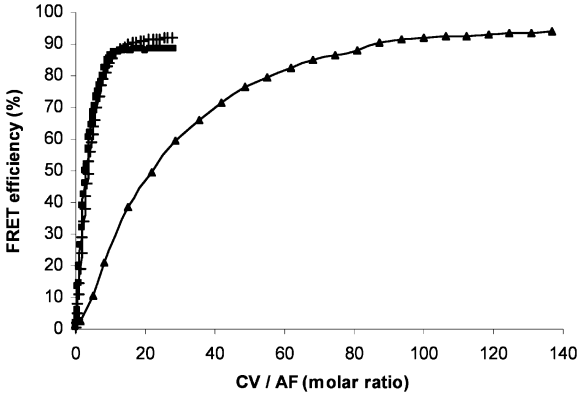

Figure 2. AF546-CV FRET efficiency versus the CV/AF546 molar ratio in solution (▲), in duplex aggregates (■), and in 10% hybridized aggregates (+). For ■ and + curves, $\lambda_{exc} = 425$ nm, $\lambda_{em} = 575$, and 638 nm. For the ▲ curve, $\lambda_{exc} = 546$ nm and $\lambda_{em} = 575$ and 638 nm.

there is a distinct difference in FRET efficiency, as a function of the CV/AF546 molar ratio, for the solutions containing labeled aggregates and that containing only the two dyes. The maximum FRET efficiency is reached at a very low CV/AF546 molar ratio (11) in the case of labeled duplex aggregates, indicating that donors and acceptors are located in close proximity to each other (i.e., within the micelles). Very similar results were obtained for duplex aggregates with and without added target DNA, indicating that the aggregated state is maintained during triplex formation. This behavior differs significantly from that of the unlabeled system, for which hybridization results in the dissolution of aggregates.

Given the micellar behavior suggested by the results above, the critical micelle concentration (cmc) of labeled aggregates was determined. To follow aggregation as a function of duplex concentration, fluorescence intensity was measured at two wavelengths: 575 nm (wavelength for maximum emission of duplex micelles) and 530 nm (wavelength for maximum emission of the free polymer). The ratio of fluorescence intensities measured at these two wavelengths should reflect the ratio of polymer within the micelles to polymer outside of them. Because duplexes are formed by stoichiometric amounts of polymer and labeled probe, concentrations of both components were varied simultaneously to obtain each data point. The same experiment was carried out for the unlabeled system. The results are plotted in Figure 3. The slopes of both curves change with increasing concentration, although no sharp discontinuity corresponding to a classic cmc is observed. The fact that there is some overlap between the emission bands of the complexed/free polymer may partially explain the absence of a sharp transition. Critical aggregation/micelle concentrations were evaluated by tracing a tangent line at the onset of the transition, and a cmc of 6.3×10^{-11} M was calculated for the labeled system, whereas a critical aggregation concentration of 2.8×10^{-9} M was obtained for the unlabeled system. The significantly lower critical concentration measured for the labeled system confirms that the self-assembly of duplex molecules into micellelike structures is promoted by the AF546.

The behavior of duplex aggregates upon dilution was also investigated, and the results are presented in Table 2 for the labeled and unlabeled systems. In the case of labeled aggregates, aggregate size remains constant, and the size distribution narrows with increasing dilution. The behavior of unlabeled duplexes is quite different, as shown by the fact that neither the size nor the particle size distribution width displays a clear trend either toward larger or smaller values with increasing dilution. This is a further

(17) Nilsson, K. P. R.; Andersson, M. R.; Inganas, O. *J. Phys.: Condens. Matter* **2002**, *14*, 10011−10020.

(18) Myers, D. *Surfaces, Interfaces, and Colloids: Principles and Applications*, 2nd ed.; Wiley-Interscience: New York, 1991.

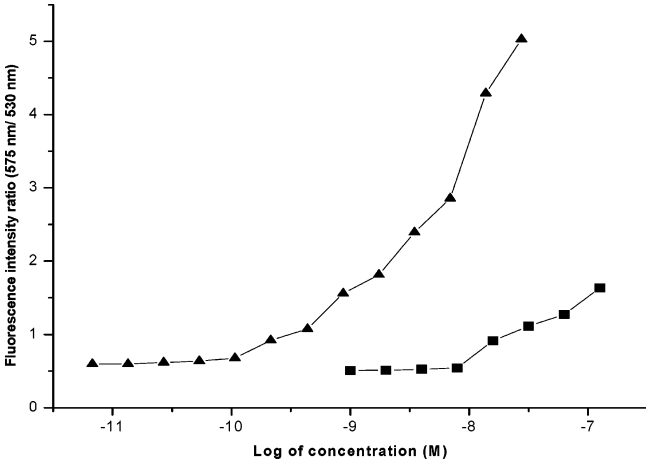

Figure 3. Evaluation of critical micelle concentration of labeled duplex aggregates (▲) and critical aggregation concentration of unlabeled duplexes (■).

Table 2. Unlabeled and Labeled Duplex Aggregate Size and Particle Distribution Width as a Function of Concentration (with Increasing Dilution) as Determined by Dynamic Light Scattering

	unlabeled duplex		labeled duplex	
concentration, M	siz,e nm	distribution width, nm	size, nm	distribution width, nm
1.00×10^{-6}			125	80
5.00×10^{-7}	190	86	123	61
2.50×10^{-7}	211	79	131	69
1.25×10^{-7}	243	97	119	49
6.25×10^{-8}	347	118	110	36
3.13×10^{-8}	293	68	123	32

indication that aggregates formed in the labeled system are micellelike because their size seems to be independent of concentration above the cmc.

The size distribution of labeled duplex aggregates in water was also measured at 65 °C at different times after formation (results not shown). Distribution profiles were found to become narrower with time, and stable aggregates of uniform size were obtained within 10 min. This behavior confirms the results of the dilution study (i.e., aggregates tend to adopt a well-defined, stable size). It is also worth noting that the size of the aggregates depends strongly on the experimental procedure used to prepare them. To obtain aggregates of a uniform size, one must mix solutions of polymer and labeled ss-DNA probes of stoichiometric concentrations ($\sim 2 \times 10^{-5}$ M) and then dilute the duplexes thus formed to the desired final concentration. Also, it has been observed that aggregates submitted to temperature stresses (formation at 25 °C, stabilization at 65 °C, and storage at 5 °C) are not uniform in size after the process and may not be able to detect DNA anymore. Thus, the characterization of aggregates by dynamic light scattering is a pivotal tool in optimizing the experimental procedure used for DNA detection.

As outlined in the Introduction section, these systems have been developed for the detection of DNA on the basis of the fluorescence changes associated with hybridization. Elucidating the effect of DNA hybridization on the micelles is therefore of crucial importance to understanding the sensing mechanism and the role of fluorophore confinement in the observed signal amplification. Interestingly, light scattering techniques were shown to be useful tools in studying supramolecular aggregates as well as surfactant mixture properties.[19−22] To investigate the

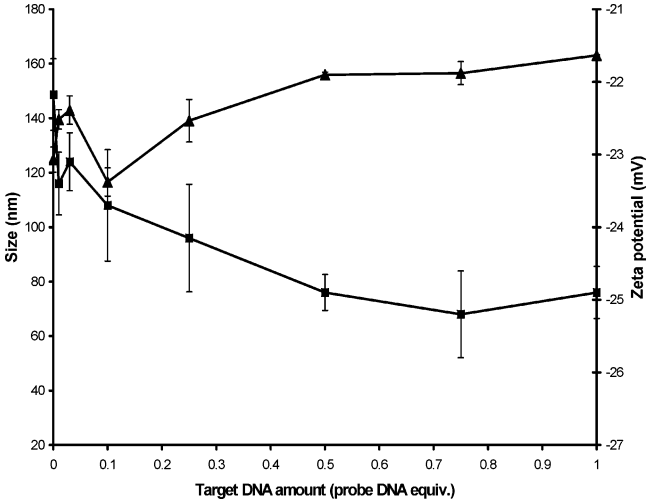

Figure 4. Hybridization of target DNA on micelles viewed by size (▲) and zeta potential measurements (■).

present sensing system, the aggregate size and zeta potential were thus measured as a function of the amount of target ss-DNA added relative to the amount of probe ss-DNA (i.e., target ss-DNA expressed in probe ss-DNA equivalents). Figure 4 shows the behavior of aggregates upon hybridization with perfectly matched target ss-DNA. At very low degrees of hybridization (below ∼0.05 in probe ss-DNA equivalents), there is an increase in aggregate size with increasing target concentration that can be attributed to the incorporation of target DNA into existing aggregates. Between 0.05 and 0.10 equiv (or 5 and 10% of added target DNA), a decrease in size is observed that might be caused by a reorganization of micelles due to an increase in electrostatic repulsion as charges are added. At 10% added target DNA and higher, the now smaller micelles can accommodate a larger number of target DNA molecules, with the result that micelle size increases further as the percentage of added target DNA reaches 100%. Note that the size increase is modest with respect to the amount of material added: at 100% hybridization, one third of the micelles are made of target DNA, so it appears that micelle reorganization occurs continuously during the process. This hypothesis is supported by zeta potential measurements, which suggest that micelles might be stabilized by the collapse in size, and further hybridization of target DNA improves their stability.

To confirm that the changes in micelles observed upon the addition of target DNA are related to specific DNA hybridization, experiments were performed to study the effect of nonspecific charges on the electrical double layer of aggregates. Because dynamic light scattering measures the hydrodynamic radius, this double layer is included in the size measurements. Also, the zeta potential is strongly influenced by the addition of salt. To visualize these effects on the micelles, we measured the changes in size and zeta potential upon an increase in ionic strength by the addition of NaCl. The amounts of NaCl added were calculated to be equivalent to the charges introduced by each DNA addition. Figure 5 shows the change in micelle size upon an increase in ionic strength, either through the addition of perfectly matched

(19) Wang, J.; Jiang, M. *J. Am. Chem. Soc.* **2006**, *128*, 3703−3708.

(20) Li, Y.; Khanal, A.; Kawasaki, N.; Oishi, Y.; Nakashima, K. *Bull. Chem. Soc. Jpn.* **2005**, *78*, 529−533.

(21) Collings, P. J.; Gibbs, E. J.; Starr, T. E.; Vafek, O.; Yee, C.; Pomerance, L. A.; Pasternack, R. F. *J. Phys. Chem. B* **1999**, *103*, 8474−8481.

(22) Moises de Oliveira, H. P.; Gehlen, M. H. *Langmuir* **2002**, *18*, 3792−3796.

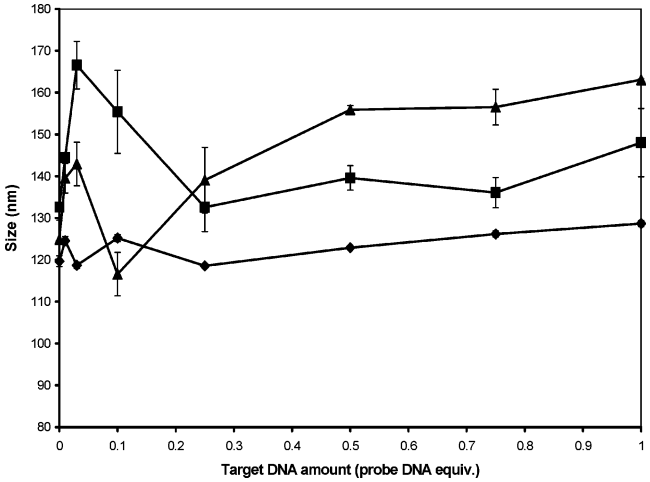

Figure 5. Size of duplex micelles upon the addition of charges either from specific DNA (▲), NaCl (■), or 1-mismatch target DNA (◆).

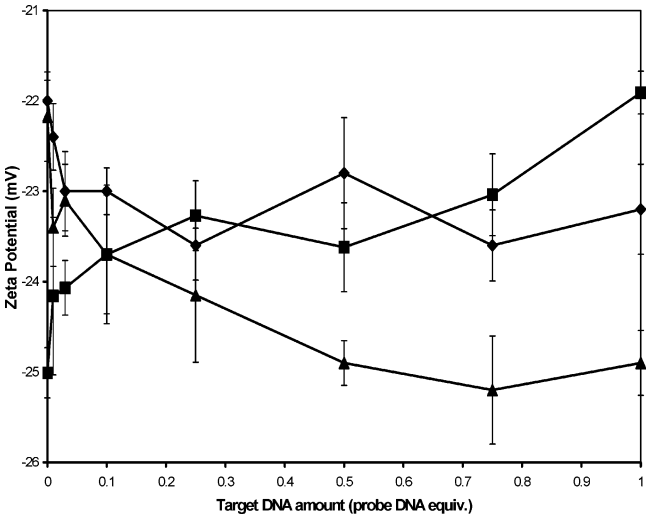

Figure 6. Zeta potential of duplex micelles upon the addition of charges either from specific DNA (▲), NaCl (■), or 1-mismatch target DNA (◆).

target ss-DNA, of NaCl, or of target ss-DNA with a single defect in its sequence (1-mismatch). The three curves show significant differences. Micelle behavior upon the addition of salt or mismatched ss-DNA is quite different from that observed upon the addition of perfectly matched target ss-DNA. Classical ionic surfactants typically exhibit an increase in micelle size at higher ionic strengths as a result of higher aggregation numbers. In the present case, the micelles are found to be larger at lower ionic strength conditions and decrease in size when the electrical double layer is compressed by incremental additions of NaCl. This decrease in size can be attributed primarily to changes in polymer conformation and micelle packing as a result of charge screening. Interestingly, the introduction of mismatched target ss-DNA does not seem to perturb the micelles, as shown by the fact that their size remains relatively unchanged during the entire process. This behavior is an indication that only perfectly matched oligonucleotides interact significantly with micelles.

The same species were studied using zeta potential measurements, and the results are shown in Figure 6. Interestingly, the zeta potential globally decreases upon hybridization with specific DNA whereas it increases upon the addition of the same number of charges from NaCl. This increase in zeta potential with an increase in ionic strength, through the addition of unspecific

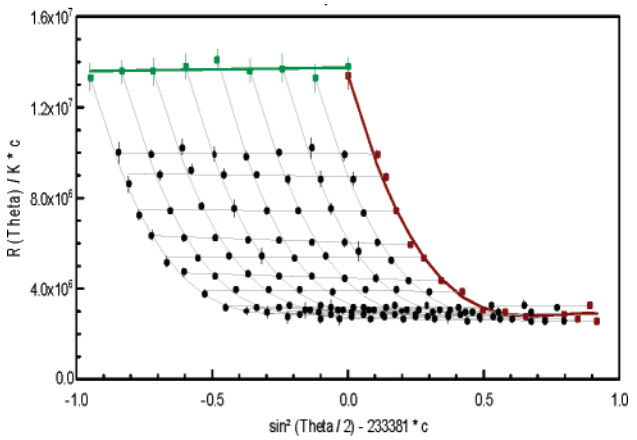

Figure 7. Debye plot obtained from MALLS measurements for labeled duplex micelles.

charges, is to be expected because the Debye length is known to decrease with increasing electrolyte concentration. However, hybridization with complementary ss-DNA results in a decrease in zeta potential. This behavior clearly indicates that specific hybridization is a distinct process that adds charges to micelles through the incorporation of target ss-DNA. In the case of mismatched target ss-DNA, there is no clear tendency, and only small fluctuations in zeta potential are observed.

It is interesting that all zeta potential measurements gave negative values for duplex aggregates, even if these entities are electrically neutral. Molecular dynamics simulations[23] were performed on a model system corresponding to a duplex formed from a 20-mer DNA sequence and the cationic polymer (20 repeating units). Preliminary results indicate that the 20-mer DNA probe is slightly longer than its associated polymer chain. This effect is attributed to the small chain torsion observed in the polymer chain, which makes it shorter and more compact when surrounded by the DNA chain. Moreover, the potential energy of the system was shown to decrease with time, suggesting a stabilization of the duplex in this configuration. The negative surface charge reported by zeta potential experiments could therefore be due to the protruding negative charges from DNA probes. To maintain the globally uncharged state of duplex aggregates, local positive charges must exist within the micelles and could promote hybridization; aggregate stabilization and the observed promotion of hybridization[10] could thus be two manifestations of this charge separation.

To construct a physical model for the labeled aggregates, the aggregate mass and corresponding aggregation number were determined by MALLS. Because the hydrodynamic diameter of the aggregates is relatively large (110 nm), the angular dependence of light scattering cannot be neglected. The refractive index increment dn/dC was determined to be +0.43 mL/g. This value is relatively high when compared to those typically determined for polymer solutions (the dn/dC of polymethymethacrylamide in water is +0.209[24]) but is consistent with a conjugated polymer in a low refractive index solvent such as water. Figure 7 shows the Debye plot obtained for our labeled aggregates. From this plot, three important parameters can be evaluated: the weight-average aggregate mass (A_M), equal to $(4.7 \pm 0.3) \times 10^7$ g/mol; the radius of gyration (R_g), equal to 116 ± 6 nm; and the second virial coefficient (A_2), equal to $(2 \pm 10) \times 10^{-5}$ mol·mL/g^2. Assuming a low polydispersity index, dividing A_M by the number-

(23) Lebouch, N.; Brisson, J.; Leclerc, M. To be submitted for publication.
(24) Huglin, M. B. *Light Scattering from Polymer Solutions*; Academic Press: New York, 1972.

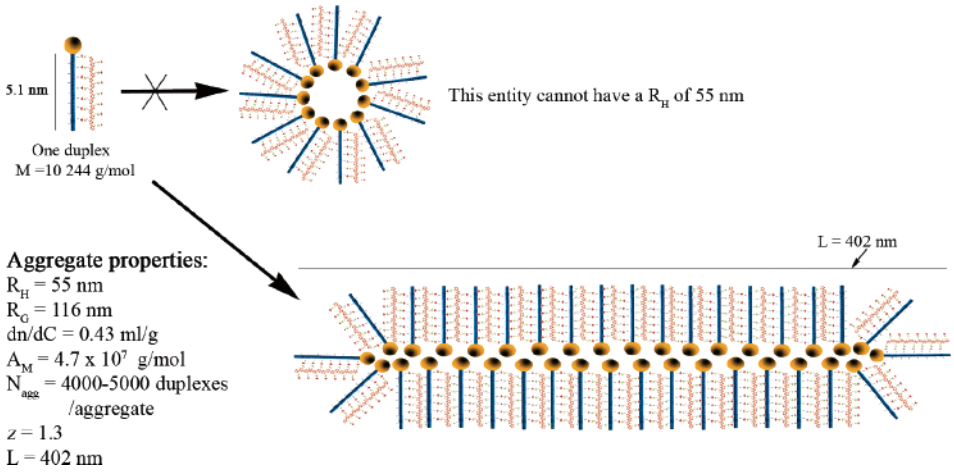

Figure 8. Proposed physical rodlike model of the labeled aggregates.

average molecular weight of a single polymer-labeled probe complex (10 244 g/mol) provides an aggregation number (N_{agg}) of ∼4000−5000 polymer−probe complexes. This number is reasonable because a relatively large number of aggregated molecules are necessary to explain the large amplification of the fluorescence signal.

The ratio of the radius of gyration to the hydrodynamic radius (R_g/R_h) is known to be a sensitive indicator of aggregate geometry.[15] In the case of labeled duplex aggregates, this ratio is equal to 2.1. Previous reports indicate an R_g/R_h ratio of 2 for well-characterized rod micelles.[13−15] For rod-shaped aggregates, the radius of gyration can also be related to aggregate dimensions by the expression $R_g^2 = L^2/12$, where L is the length of the rod.[25] For duplex micelles, a rod length of 402 nm can be calculated in this way. Finally, the shape of a scattering entity can also be evaluated from the dissymmetry ratio (z), defined as the ratio of the scattering intensity at two complementary angles ($i_{45°}/i_{135°}$). The value of z at a given characteristic size parameter (L/λ in the present case, where λ is the radiation wavelength in vacuum (632.98 nm) divided by the refraction index of the scattering medium ($n_{water} = 1.33$)) differs significantly for spheres, rods, and coils. MALLS measurements yield values of z and L/λ equal to 1.3 and 0.84, respectively, which place this system in the rod conformation region.[25] A rod model for the labeled aggregates is therefore consistent with our results as well as with the fact that, given the size of the constituent molecules, it would be impossible to form a spherical micelle with a single hydrophobic core and having the dimensions given by the light scattering measurements. The polymer−probe duplex has approximately the same dimensions as ds-DNA, which has a radius of 9.5 Å and a length of 3.4 Å per base[26] for a total length of ∼ 5.1 nm. One can easily see that a simple spherical micelle formed with these constituents cannot have a hydrodynamic radius of 55 nm. Figure 8 presents the schematic representation of a rod micelle arrangement having the dimensions given by the light scattering measurements of labeled duplex aggregates. Furthermore, TEM images taken of duplex and triplex aggregates deposited on TEM grids (Figure 9) substantiate the rod micelle model described above (i.e., the dimensions of the rod-shaped structures observed by TEM are very similar to those that were calculated using light scattering measurements; see Supporting Information).

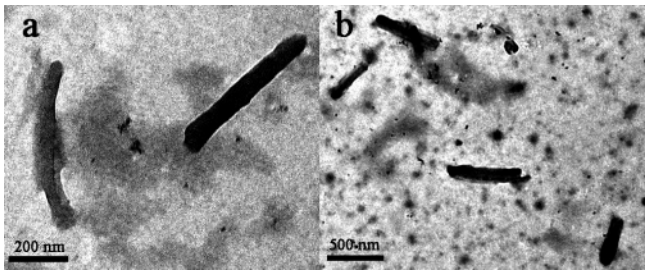

Figure 9. TEM images of labeled aggregates: (a) duplex aggregates and (b) 10% hybridized aggregates.

Conclusions

We have shown that a cationic polythiophene complexed with labeled or unlabeled DNA probes forms supramolecular aggregates that possess fluorescence properties that are closely related to their aggregation properties. For the unlabeled system, the fluorescence intensity of the complexes is inversely proportional to the scattered light intensity. In the duplex form, when charges are neutralized by the DNA probe, polymer chains are in a planar conformation and nonfluorescent aggregates are formed; when free in solution or complexed with ds-DNA, polymer chains adopt a random coil or helical conformation, respectively, both of which are highly soluble.[4] For the labeled system, high quantum yield, photostability, and FRET efficiency values hinge on the conservation of an aggregated state upon hybridization.[12] FRET measurements using an acceptor dye with a charged molecular structure similar to that of AF546 support the micellar nature of labeled aggregates, as does the observation of a slight increase in aggregate size with increasing temperature. Fluorescence measurements also helped us to evaluate the critical micellar and aggregate concentrations of the labeled and unlabeled aggregates to be 6.3×10^{-11} and 2.8×10^{-9} M, respectively. Dynamic light scattering measurements highlighted the fact that labeled micelles tend to adopt a definite size, and it has been noticed that the size distribution widths become narrower with either time or dilution.

In addition, studies of micelle hydrodynamic size and zeta potential as a function of the amount of perfectly matched DNA, 1-mismatch DNA, or NaCl added also contributed to the elucidation of micelle behavior. During the hybridization of specific ss-DNA targets, micelle size changes to accommodate the charges carried by target ss-DNA, whereas the addition of 1-mismatch target ss-DNA or NaCl does not have this effect. Zeta potential measurements support this interpretation and

(25) Hiemenz, P. C.; Rajagopalan, R. *Principles of Colloid and Surface Chemistry*, 3rd ed.; Marcel Dekker: New York, 1997.
(26) Halperin, A.; Buhot, A.; Zhulina, E. B. *Biophys. J.* **2004**, *86*, 718−730.

suggest that the nature of the target greatly influences the stability of the micelles because it was observed that the addition of charges only from specific ss-DNA increases their stability.

Furthermore, to obtain more information about the molecular structure of these aggregates, MALLS experiments were performed. An aggregate mass of $(4.7 \pm 0.3) \times 10^7$ g/mol was calculated, which indicates an aggregation number (N_{agg}) of ~4000−5000 duplexes/aggregate. This number is consistent with previous fluorescence results.[10] Moreover, the measurement of z and R_g/R_h pointed toward a rod micelle model for the labeled duplex aggregates, a hypothesis confirmed by TEM images of rod-shaped micelles of approximately 400 nm in length. This new physical model will be of great help in visualizing the molecular and photophysical processes that happen within these promising DNA-responsive aggregates.

Acknowledgment. We thank M. Viger for help with TEM imaging, N. Lebouch for molecular dynamics simulations, Cédric Plesse and Hoang-Anh Ho for the synthesis of the polythiophene, as well as the Natural Sciences and Engineering Research Council (NSERC) of Canada for financial support. K.D. acknowledges the NSERC for a Ph.D. scholarship.

Supporting Information Available: AFM images of labeled duplex aggregates. This material is available free of charge via the Internet at http://pubs.acs.org.

LA061699A